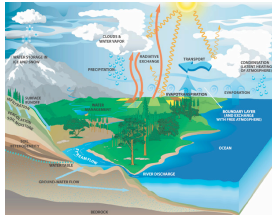


# Precipitation and Latent Heating Distributions Derived from Active and Passive Microwave Observations

William Olson<sup>1</sup>, Mircea Grecu<sup>2</sup>, Tristan L'Ecuyer<sup>3</sup>, Michael Bosilovich<sup>4</sup>, Chung-Lin Shie<sup>2</sup>, and Wei-Kuo Tao<sup>4</sup>

1: Joint Center for Earth Systems Technology/Univ. Maryland Baltimore County; 2: Goddard Earth Sciences and Technology Center/Univ. Maryland Baltimore County; 3: Colorado State University; 4: NASA/Goddard Space Flight Center

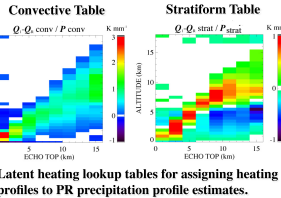
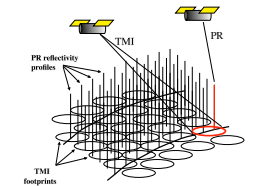
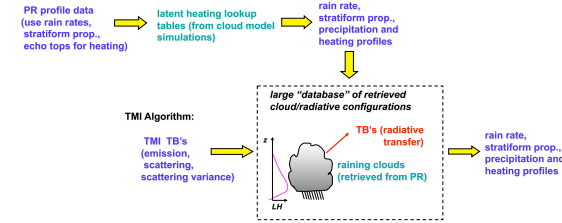


**Why?** to better understand the global hydrologic and energy cycles and the dynamics associated with latent heat release. Precipitation flux is a key component of the water cycle linking the atmosphere and oceans/land surfaces at a rate of approximately 2.6 mm day<sup>-1</sup>. Globally, this precipitation flux is balanced by evaporation and evapotranspiration that represent a consumption of the sun's energy to move liquid-phase water molecules to the vapor phase. Atmospheric circulations move the water vapor, which carries the sun's energy in the form of latent heat, to regions of convergence where the vapor condenses and the latent heat is released to the atmosphere at a rate of about 76 W m<sup>-2</sup>, globally. Regions of higher precipitation and latent heating, particularly in the tropics, are associated with the rising branches of global-scale atmospheric circulations. Therefore, variations of the large-scale patterns of precipitation and latent heating modulate atmospheric dynamics, which in turn have an impact on the distributions of precipitation in both the tropics and extra-tropics. By quantifying the 4D distributions of precipitation and latent heating using a series of estimates derived from low earth-orbiting satellite microwave radiometer observations, we hope to provide useful diagnostics for global climate model simulations and, in addition, possible assimilation products for climate models.

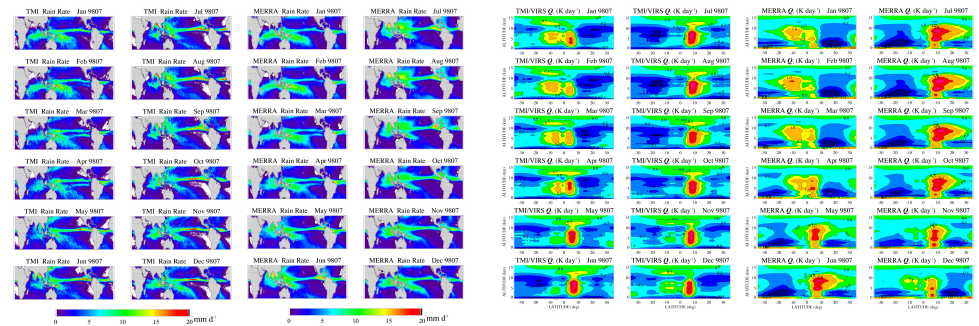
## Precipitation and Latent Heating ( $Q_1$ - $Q_R$ ) Estimation Method

The precipitation/latent heating estimation algorithm combines information from the spaceborne Precipitation Radar (PR) and TRMM Microwave Imager (TMI), which are both operating on the Tropical Rainfall Measuring Mission (TRMM) satellite. The PR provides precipitation structure information at relatively high vertical and horizontal resolution, while the TMI, being a passive instrument, provides information related to the vertical integrals of liquid- and ice-phase precipitation. Therefore, it follows that the PR should provide more specific information on latent heating, which is related to precipitation structure. However, the PR provides only about 1/3 the sampling of the TMI, and since there will only be one scanning weather radar in space at any time, while several satellite microwave radiometers will continue to be operational from now to the foreseeable future, we developed an algorithm for estimating precipitation/latent heating from TMI that uses PR heating estimates as "training" data. Below is a schematic of the "TRAIN" algorithm:

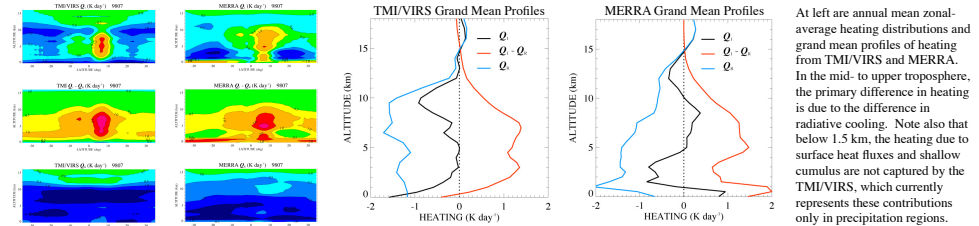
### PR "Training" Algorithm:



## Preliminary MERRA Comparisons



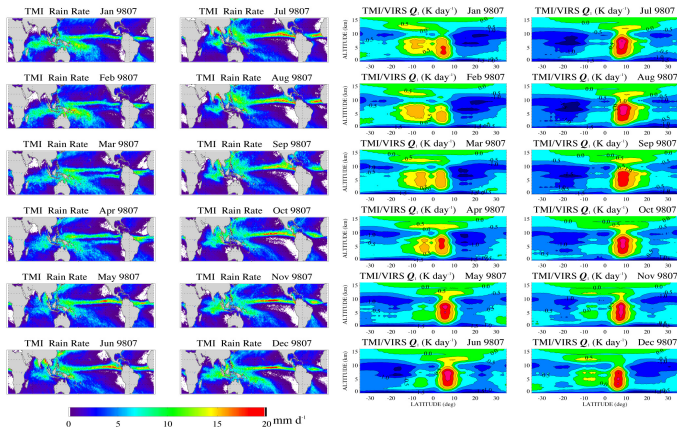
The Modern Era Retrospective-Analysis for Research and Applications (MERRA) utilizes the GEOS5 model, developed at NASA Goddard's Modeling and Assimilation Office to assimilate conventional observations as well as satellite radiance information to produce a long-term record (1979 – present) of the evolution of the Earth's atmosphere. The overarching objective of MERRA is to "provide the science and applications communities with state-of-the-art global analyses, with emphasis on improved estimates of the hydrological cycle on a broad range of weather and climate time scales". Here we compare the 10-year (1998 – 2007) average estimates of precipitation and latent heating over ocean from TMI/VIRS to the corresponding MERRA reanalysis products. The monthly-mean precipitation fields (above left) from TMI and MERRA show good consistency through the seasonal cycle. Note, however, that in comparisons between the Global Precipitation Climatology Project (GPCP) precipitation product and MERRA, there is a ~0.5 mm day<sup>-1</sup> high bias of MERRA relative to GPCP in the third reanalysis stream (1998 – present) over tropical oceans. Plots of zonal-average  $Q_1$  from TMI/VIRS and MERRA are shown above right. Although the seasonal shift of the heating distribution can be seen in both products, there is significantly greater mid- to upper-tropospheric heating associated with deep convection in the MERRA reanalysis. Greater lower-tropospheric radiative cooling outside the convective maximum regions is also evident in the MERRA product.



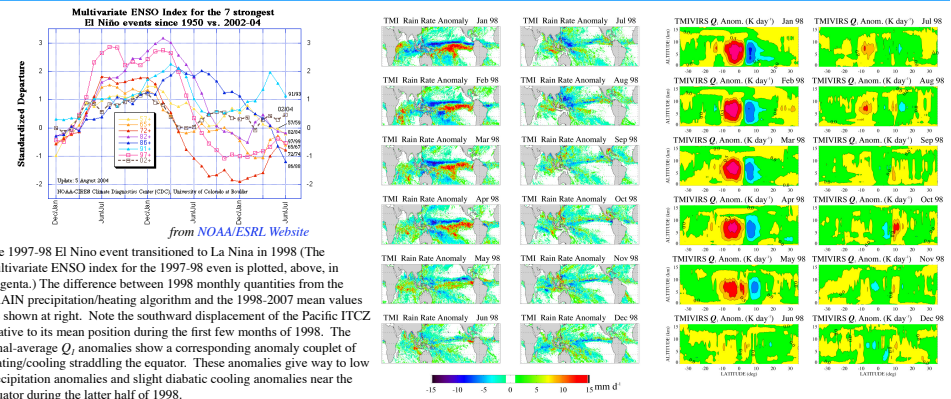
At left are annual mean zonal-average heating distributions and grand mean profiles of heating from TMI/VIRS and MERRA. In the mid- to upper troposphere, the primary difference in heating is due to the difference in radiative cooling. Note also that below 1.5 km, the heating due to surface heat fluxes and shallow cumulus are not captured by the TMI/VIRS, which currently represents these contributions only in precipitation regions.

## 1998-2007 Mean Seasonal Cycles of P, Zonal-Average $Q_1$

We constructed an estimate of the apparent heat source ( $Q_1$ ) by adding our TRAIN estimates of  $Q_1 - Q_2$  from TMI to Tristan L'Ecuyer's estimates of  $Q_2$  from TMI/VIRS (HERB algorithm). As a demonstration, the 1998-2007 mean seasonal cycle of estimated surface rain rates and zonal-average  $Q_1$  are shown at right. The seasonal movement of the ITCZ/monsoons, following the subsolar point, is evident in the maps of mean monthly precipitation at above left. The corresponding zonal-average diabatic heating is dominated by latent heat release in the deep tropics, with movement about the heating maximum at ~5-10 °N. Note the strong latent heating/radiative cooling couplets that occur in January and July, with radiative cooling located in the winter hemisphere. These couplets are consistent with asymmetric structure of the Hadley circulation at the solstices, with the rising branch of the circulation near the maximum of latent heating and the descending branch in the winter hemisphere, corresponding to the maximum of radiative cooling; see, e.g., Peixoto and Oort, *Physics of Climate*, 1992.



## 1998 Precipitation / Zonal-Average $Q_1$ Anomalies



The 1997-98 El Niño event transitioned to La Niña in 1998 (The multivariate ENSO index for the 1997-98 event is plotted, above, in magenta.) The difference between 1998 monthly quantities from the TRAIN precipitation/heating algorithm and the 1998-2007 mean values are shown at right. Note the southward displacement of the Pacific ITCZ relative to its mean position during the first few months of 1998. The zonal-average  $Q_1$  anomalies show a corresponding anomaly couplet of heating/cooling straddling the equator. The anomalies give way to low precipitation anomalies and slight diabatic cooling anomalies near the equator during the latter half of 1998.